Construction and Building Materials 162 (2018) 704–713

Contents lists available at ScienceDirect

Construction and Building Materials

journal homepage: www.elsevier.com/locate/conbuildmat

Experimental study on seismic behaviors of concrete columns confined by corroded stirrups and lateral strength prediction

Li Qiang [a,*], Niu Di-tao [b], Xiao Qian-hui [a], Guan Xiao [a], Chen Shao-jie [a]

[a] Department of Civil Engineering and Architecture, Xi'an University of Science and Technology, Xi'an 710054, China
[b] Department of Civil Engineering, Xi'an University of Architecture & Technology, Xi'an 710054, China

HIGHLIGHTS

- Low-reversed cyclic loading tests were carried out on eight corroded reinforced concrete columns to study their mechanical characteristics and failure mechanisms. The test results are analyzed in detail, and the research on the decline in the seismic performance of concrete columns confined by corroded stirrups has been carried out for the first time.
- A method for predicting the lateral strength of reinforced concrete columns confined by corroded stirrups is presented based on the axial-shear-flexure interaction approach for conventional concrete columns, with modifications to consider the effect of stirrup corrosion. There was good agreement is achieved between the test results and theoretical values. For the first time, the established model introduces the corrosion parameters of the stirrup.

ARTICLE INFO

Article history:
Received 10 January 2017
Received in revised form 4 September 2017
Accepted 8 September 2017

Keywords:
Corroded stirrup
Low reversed cyclic loading
The key parameter
Seismic performance
The axial-shear-flexure interaction approach

ABSTRACT

To understand the seismic behaviors of concrete columns confined by corroded stirrups, low-reversed cyclic loading tests were carried out on eight corroded reinforced concrete columns to study their mechanical characteristics and failure mechanisms. The influence on seismic performance indicators such as bearing capacity, hysteresis characteristics, ductility, strength degradation, stiffness degradation, and energy dissipation was analyzed comparatively based on parameters such as stirrup diameter and stirrup-spacing changes. The experimental results showed that the restraint of concrete provided by corroded stirrups is reduced, which leads to a decline in seismic performance, and with increasing stirrup corrosion, the failure limit displacement of columns decreases. The pinch phenomenon of the hysteresis curve gradually increases, the attenuation degree of strength and stiffness increases, and the ductility and energy-dissipation capacity is reduced, while the accumulated energy increases under the same control displacement. A method for predicting the lateral strength of reinforced concrete columns confined by corroded stirrups is presented based on the axial-shear-flexure interaction approach for conventional concrete columns, with modifications to consider the effect of stirrup corrosion. There was good agreement is achieved between the test results and theoretical values.

1. Introduction

Traditional architectural design and construction management systems consider each stage of building separately. In many structures, this results in serious defects, poor performance, low durability, and short service life among other things. Consistent with the life-cycle concept, estimates of durability and residual life have become an important research area of structural engineering [1–4].

Due to long-term effects of carbonation, freeze-thaw cycles, and other factors, reinforcements in concrete structures will exhibit different degrees of corrosion damage, which leads to degradation of structural bearing capacity and ductility, and serious corrosion will threaten the security of a structure. Therefore, the degradation of concrete structures due to corrosion cannot be ignored. Progress has been made in the study of the seismic performance of reinforced concrete columns subject to corrosion [5–7]. Corrosion in the joint part of the stirrups and their transverse reinforcement is rather serious, but the effect of stirrup corrosion has been ignored. Not only does the established restoring force model not introduce the parameters of stirrup corrosion, but the preexisting analysis of the mechanism of the decline in seismic performance after stirrup corrosion has not been carried out. After a stirrup corrodes, its mechanical performance and confinement of the core

* Corresponding author.
E-mail address: liguanqiang2005@126.com (Q. Li).

https://doi.org/10.1016/j.conbuildmat.2017.09.030
0950-0618/

concrete and transverse reinforcement decline, which leads to a decrease in the bearing capacity and stiffness of reinforced concrete columns and a change in the failure pattern from ductile fracture to brittle failure, which could even lead to the sudden collapse of a structure. Therefore, the degradation effect of stirrup corrosion on the bearing capacity of reinforced concrete columns is greater than that of the corrosion of transverse reinforcement. The study of the influence of stirrup corrosion on mechanical performance of concrete columns has just begun, and research on the decline in the seismic performance of concrete columns confined by corroded stirrups has not been carried out.

In this paper, low-reversed cyclic loading tests have been carried out for eight corroded reinforced concrete columns to study their mechanical characteristics and failure mechanisms. The influence on seismic performance indicators such as bearing capacity, hysteresis characteristics, ductility, strength degradation, stiffness degradation, and energy dissipation have been analyzed comparatively using parameters such as stirrup diameter and stirrup spacing. A lateral strength-prediction method is proposed for reinforced concrete columns confined by corroded stirrups.

2. Test survey

2.1. Model design and production

The comparison test designed eight reinforced concrete columns, whose thickness of the concrete cover is 15 mm. The section size and reinforcements are shown in Table 1.

Specimens were cast by pouring them into molds in wooden templates. To avoid transverse reinforcement corrosion, measures were taken to isolate the transverse reinforcement and stirrups, and a wire with a 4-mm diameter was connected to the corroded stirrups. They were vertically cast to ensure unique concrete specimens.

2.2. Material performance

The design strength of concrete Specimens is C25, and the basic performance is shown in Table 2. Specimens' transverse reinforcements using HRB335 steel, stirrups using HPB235 steel, the basic mechanical performance is shown in Table 3.

2.3. The corrosion rate of specimen' stirrups

The numerical corrosion rate is the average stirrups' corrosion rate within the scope of bottom plastic hinge area. The numerical corrosion rate of all specimens is shown in Table 4.

Table 1
Dimensions and reinforcement of specimens.

Specimen	Size/mm	Reinforcement/mm	Stirrup/mm
RC-1	200 × 200	6ϕ14	ϕ8@70
RC-2	200 × 200	6ϕ14	ϕ8@70
RC-3	200 × 200	6ϕ14	ϕ8@70
RC-4	200 × 200	6ϕ14	ϕ8@70
RC-5	200 × 200	6ϕ14	ϕ8@90
RC-6	200 × 200	6ϕ14	ϕ8@90
RC-7	200 × 200	6ϕ14	ϕ8@120
RC-8	200 × 200	6ϕ14	ϕ8@120

Table 2
Fundamental properties of concrete and blocks.

Material types	Bulk density/ kN/m^3	Compressive strength/ MPa	Elastic modulus/ MPa
C25	33.85	50.3	3.0×10^4

Table 3
Basic mechanical properties of reinforcement.

Grade	Diameter	Yield strength	Ultimate strength	Elastic modulus	Elongation
HPB235	8 mm	292 MPa	515 MPa	2.19×10^5	25.6%
HRB335	14 mm	359 MPa	552 MPa	1.97×10^5	18.8%

Table 4
Stirrups corrosion rate of all specimens.

Component	Average weight loss rate	Maximum weight loss rate
RC-1	0	0
RC-2	4.76%	4.76%
RC-3	12.90%	30.65%
RC-4	22.22%	46.49%
RC-5	9.23%	36.53%
RC-6	13.96%	46.87%
RC-7	15.55%	34.49%
RC-8	16.69%	48.39%

2.4. Test method and loading system

Seismic test methods [8,9] were used in the low-reversed cyclic loading test, and cantilever loading equipment was adopted, as shown in Fig. 1.

A vertical load with a fixed value of 200 kN was applied to the top of the column by a jack.

The horizontal load was applied to the upper column by means of a reaction frame with the help of hydraulic actuators.

The loading mechanism used a force-displacement hybrid control. First, the yield adopted the load-control and step-loading method; each stage of loading was 10 kN, and each stage was repeated once. After adopting displacement control, the amount of each displacement increase was a multiple of the yield displacement, and each stage of displacement was repeated three times, with the test terminating when the specimen could not bear axial pressure. The test loader is shown in Fig. 2.

3. Experimental results and analysis

3.1. Failure mode and mechanism analysis

The damage to all specimens occurred at the bottom plastic hinge area of the column, which experienced elastic, elastic-plastic, and failure stages. The ultimate destruction is shown in Fig. 3. To summarize, before the horizontal load reaches 40% of the ultimate load, the column is in the elastic state, where the load curve and the unloading curve coincide to a straight line. When the load reaches 60–70% of the ultimate load, minor cracks appear in the roots, and surface cracks of the component develop continuously with the increase of the horizontal load. When the load reaches 80–90% of the ultimate load, concrete cracks develop rapidly, and the concrete cover falls off gradually. At the ultimate stage, the external drum of reinforcements appears at the root of the specimen, the core area of the concrete is crushed, and members cannot bear the horizontal load.

The major damage feature points of each component, distribution of load steps, and surface-crack morphology during the test are shown in Table 5, and the final failure modes are shown in Table 6.

Table 5 shows that the loading step of each failure characteristic point of RC-2 is the same for RC-1, but the loading step of final destruction is postponed longer for RC-2 than for RC-1. This is because the bond between stirrups and concrete becomes stronger when the stirrups corrode slightly, which not only improves the

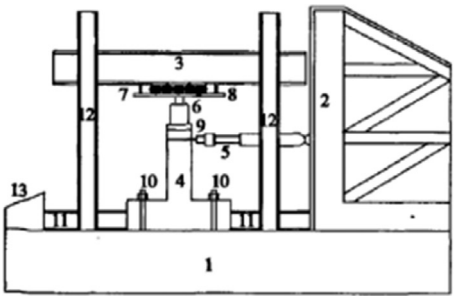

Fig. 1. Loading device of reinforced concrete column.

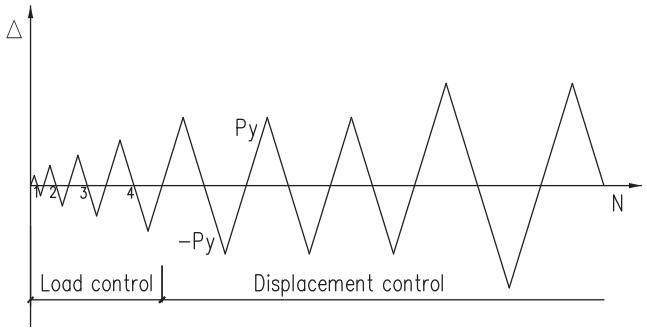

Fig. 2. The loading program of test.

bearing capacity of the component to a certain extent but also improves the ductility. The loading step of each failure characteristic point and final destruction of other relatively seriously corroded components are all ahead of RC-1. This indicates that the damage of concrete cover and the degradation of confined performance to core concrete caused by corroded stirrups result in declining bearing capacity and ductility.

Table 6 shows that RC-1 and RC-2 appear to have the better ductility bending failure. As the amount of stirrup corrosion increases, the ability to confine the core concrete is weakened by corroded stirrups, and the contribution of corroded stirrups to the specimen of shear bearing capacity is reduced. So, the failure mode of members gradually shifts to brittle failure. A clear shear failure surface is formed at the root of the plastic hinge zone, while the stirrups' failure mode changes from a slight deformation to external drum even pull off, the core concrete crushing, transverse reinforcement buckling in a lantern shape. Stirrup corrosion causes the concrete cover to become damaged and fall off after transverse reinforcements yield. This is because the accumulation of corrosion products close to the stirrup cross-section damages the binding between the concrete cover and concrete in the core area, with the damage becoming more severe as the degree of stirrup corrosion increases.

3.2. Hysteresis curve

Hysteresis curves [11,12] that reflect the characteristics of structural deformation, rigidity degradation, and energy dissipation in the process of repeated stress are used to determine the restoring force model and the basis of nonlinear seismic response analysis. The hysteresis curves of eight concrete columns under low-reversed cyclic loading are shown in Fig. 4.

Some conclusions can be reached from Fig. 4:

(1) The central component of the hysteresis curve that appears obviously to be a "pinch approach" phenomenon is a typical curved-scissors model of a hysteresis curve, and the hysteresis curves are greatly influenced by the shear deformation.
(2) Before the transverse reinforcement yields, the hysteresis curve of each component is narrow and long, residual deformation is small, the area of the hysteresis loop back is smaller with less energy dissipation, the stiffness of integral components show little change, and the values of load and displacement are basically symmetrical.
(3) After the transverse reinforcement yields, the hysteresis curve of each component tracks toward the displacement axis, and the area of the hysteresis loop back and energy dissipation gradually increase. In the loading stage of the same displacement, the bearing capacity and stiffness of two later cycles are lower than in the first cycle, which shows that the strength, stiffness, and energy-dissipation capacity of reinforced concrete columns are degenerate. But energy dissipation increases with increasing cycling times, which reflects the influence of the cumulative damage.

(a) RC-1 (b) RC-2 (c) RC-3 (d) RC-4 (e) RC-5 (f) RC-6 (g) RC-7 (h) RC-8

Fig. 3. Failure pattern of concrete column confined by the corroded stirrups.

Table 5
Basic mechanical properties of reinforcement.

Component	Crack load	Fracture shape		Crack load step	Crossing crack load step	Concrete cover falling load step	Ultimate loading step
		Load application side	The other side				
RC-1	+5t	Change at Corner horizontal fractures to oblique fractures	Horizontal fractures	+20 mm①	−30 mm③	+30 mm③	−60 mm①
RC-2	−4t	Change at Corner horizontal fractures to oblique fractures	Horizontal fractures	+20 mm①	−30 mm③	+30 mm③	+60 mm③
RC-3	+4t	Horizontal cracks and vertical cracks mainly	Horizontal fractures	−6 t	−6 t	−20 mm①	+60 mm①
RC-4	+4t	Horizontal cracks and vertical cracks are main	Horizontal fractures	+10 mm①	+10 mm①	+20 mm①	−50 mm①
RC-5	+4t	Oblique fractures mainly	Horizontal fractures	+10 mm①	+20 mm①	+20 mm③	−50 mm①
RC-6	−3t	Oblique fractures mainly	Horizontal fractures	+10 mm①	+20 mm①	+20 mm③	+50 mm③
RC-7	+4t	Corner vertical fractures mainly	Corner vertical fractures and horizontal fractures	+10 mm①	−20 mm①	+20 mm③	−40 mm①
RC-8	+4t	Corner vertical fractures mainly	Corner vertical fractures and horizontal fractures	+10 mm①	−20 mm①	−20 mm①	+40 mm②

Note: "+" indicate push loading, "−" indicate tension load. ①, ②, ③ represent the first second and third cycle of loading step respectively.

Table 6
The failure pattern of reinforced column.

Component	Failure mode	Angle of shear failure plane	Failure mode of stirrup	Failure mode of transverse reinforcement
RC-1	Bending failureare mainly	–	No fracture, deformation is not significant	Buckle between the first and second stirrup in bottom
RC-2	Bending failureare mainly	–	The first stirrup in bottom is convex	Buckle between the first and second stirrup in bottom
RC-3	Bending and shearing failures	About 60°	The first second and third stirrups in bottom are convex	Buckle between the first and third stirrup in bottom
RC-4	Shear failure mainly	About 60°	The first and second stirrups fracture in bottom	Buckle between the first and second stirrup in bottom
RC-5	Shear failure	About 60°	The second stirrup in bottom deformed obviously	Buckle slightly between the first and second stirrup in bottom
RC-6	Shear failure	About 55°	The first stirrup deformed seriously, stirrup in the crook removed	Buckle at the first stirrup in bottom
RC-7	Shear failure	About 65°	Stirrups deformed slightly	Buckle slightly between the first and second stirrup in bottom
RC-8	Shear failure	About 70°	The second stirrup fractured	Collapse between the first and third stirrup in bottom

(4) After the peak load, the capacity declines are relatively flat and hysteresis curve areas continue to increase. However, for components with the same stirrup spacing, the degree of decline of bearing capacity increases with the increase of the stirrup-corrosion rate.
(5) When components are damaged, the hysteresis curves of RC-1 and RC-2 are relatively full, the "pinch approach" phenomenon is not obvious, and they show good plastic deformation and energy-dissipation capacity. The hysteresis curves of RC-3 and RC-5, which is corroded slightly, show a slight "pinch approach" phenomenon. The hysteresis curves of RC-4, RC-7, and RC-8, which are corroded seriously after transverse reinforcement yields, show obvious "pinch approach" phenomena, and their deformation capacity and energy-dissipation capacity are decreased significantly.
(6) With smaller stirrup spacing, the pinch approach phenomenon of the hysteresis curve is not obvious, hence we conclude that member ductility increases with the decrease of stirrup spacing. So, the pinch approach phenomenon of the hysteresis curve is not only related to the degree of stirrup corrosion, but also to the stirrup spacing.
(7) Specimens whose stirrup spacing is 70 mm: The stirrup corrosion rate of RC-2 is smaller, which is related to the corrosion accumulation felt at the gaps between the stirrups and concrete; the bearing capacity of RC-2 at various stages is improved, and the hysteresis curve is relatively fuller. The stirrup-corrosion rate of RC-3 is relatively serious, from the start of loading to control displacement of 20 mm of the cyclic loading stage, whose stiffness is not significantly less compared with RC-1; there is a slight increase instead, and the earlier the loading stage, the more obvious the increase, which is related to the corrosion accumulation felt by the gaps between stirrups and concrete. The stirrup corrosion rate of RC-4 is the most serious. The concrete cover is basically out of work, the confinement to core concrete by corroded stirrups is degraded, and the bearing capacity and stiffness gradually diminish, with the degree of the degradation increasing as the control displacement increases. Under the same displacement, the bearing capacity and stiffness of all specimens are reduced more obviously with the increase of the stirrup-corrosion rate.
(8) Specimens whose stirrup spacing is 90 mm or 120 mm: The stirrup corrosion of all specimens is more serious, the bearing capacity and stiffness decrease gradually during all stages of cyclic loading, and the degree of reduction increases as the controlled displacement and stirrup-corrosion rate increase.

3.3. Skeleton curve

A skeleton curve is the envelope of all cycle peaks during the low cyclic loading test. This can accurately reflect the seismic performance of strength, deformation, and ductility, and provides an important basis to determine the feature points of a restoring force

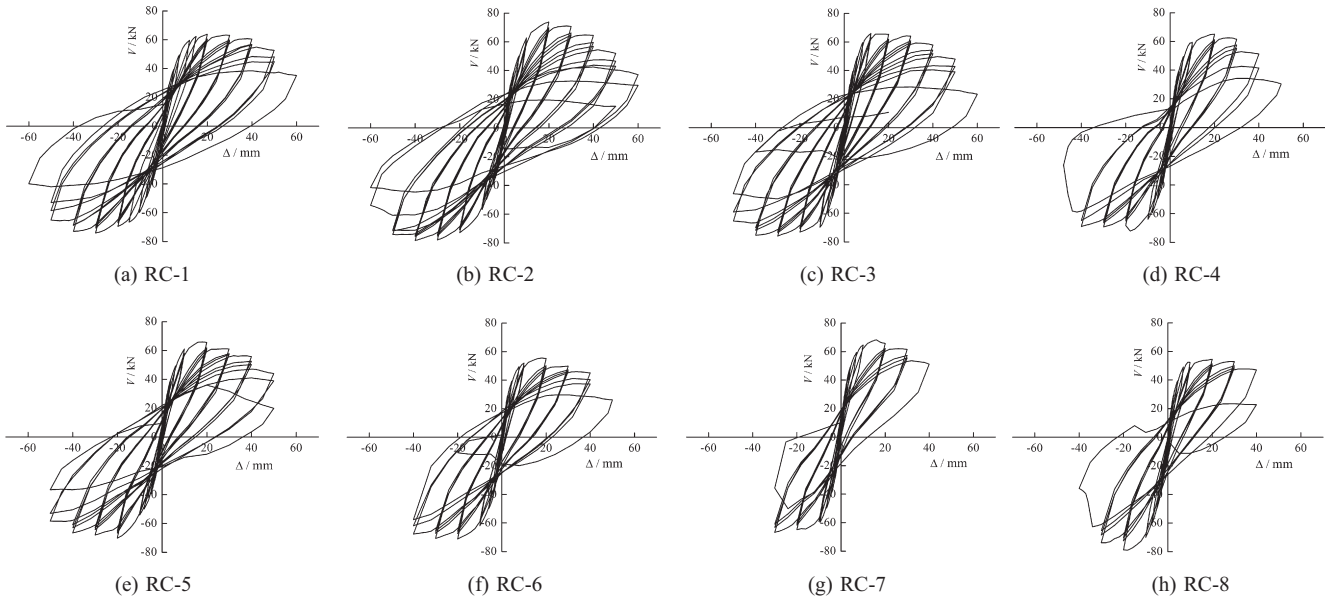

Fig. 4. Hysteresis curve of the corroded columns.

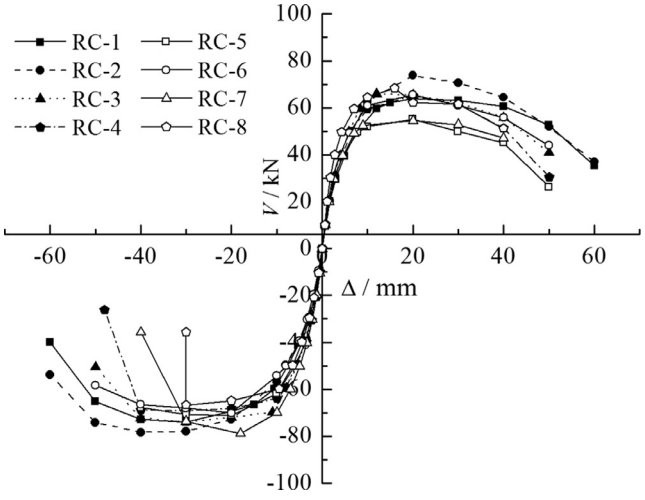

Fig. 5. Skeleton curve of the corroded column.

model. The contrast skeleton curves of all specimens are shown in Fig. 5.

Some conclusions can be drawn from Fig. 5:

(1) The stress process of all specimens shows elastic, elastic-plastic, and destruction stages.

(2) Specimens with stirrup spacing of 70 mm: ①When the horizontal load is less than 20 kN, the lateral displacement of each component is small, and the skeleton curves coincide, which shows that concrete cover damage and corrosion of stirrups did not have an obvious influence on the elastic stage performance. When the horizontal load is more than 20 kN, the difference between the skeleton curves before transverse reinforcement yield gradually emerges, which shows that the impact of the concrete cover damage and corrosion of stirrups on specimens' performance has begun to appear. ②When the horizontal displacement was less than 50 mm, the horizontal load of RC-2 was greater than that of RC-1, which shows that slightly corroded stirrups are good for shear capacity. When the specimen is close to failure, the concrete cover is out of work completely, and bond-slip between stirrups and concrete will be produced; the products lose these favorable effects of corrosion products, and the horizontal loads of RC-2 and RC-1 are basically the same. ③When the horizontal displacement is less than 30 mm, the horizontal loads of RC-3 and RC-4 are greater than that of RC-1 under the same displacement, indicating that the shear capacity has not declined because of the cracking of the concrete cover and the confinement effect due to the corroded stirrups. It is improved because of the relative motion on both sides of the concrete crack in the process of the low-reversed cyclic loading. ④When the displacement is more than 30 mm, RC-3 and RC-4 have smaller horizontal loads than RC-1 under the same displacement, and the degradation of the horizontal load is more obvious with increased stirrup corrosion. This shows that when stirrup corrosion is serious, the confinement performance on the core concrete is weakened by corroded stirrups, significantly reducing the ability to resist horizontal loads.

(3) Specimens with stirrup spacing of 90 mm and 120 mm: ①When the horizontal load is less than 10 kN, lateral displacement of each specimen is small, and the skeleton curves of all specimens are basically coincident. When the horizontal load is more than 10 kN, the differences between the skeleton curves are gradually revealed. ②In the low-reversed cyclic loading test, the horizontal load of specimens with seriously corroded stirrups is less than that when stirrups are corroded relatively slightly. The difference is more obvious after yielding of transverse reinforcement.

3.4. Intensity attenuation

In the low-reversed cyclic loading test, the damage continues to accumulate, and the mechanical properties of the structure and structural members will degrade with the increase of the control load and displacement. The intensity attenuation ζ is one of the important macroscopic quantities reflecting this degradation. To study the influence of different parameters on the strength attenuation of reinforced concrete columns and to accurately assess their ability to external load of specimens, the relation curves of

specimens' intensity attenuation and corrosion amount and spacing of stirrups are shown in Figs. 6 and 7, respectively.

From Figs. 6 and 7, we can learn the following about the strength attenuation of members:

(1) The trend of intensity attenuation of each specimen increases with increases of the stirrups' weight loss and lateral displacement, mainly because the restraint to the core concrete by stirrups is more obvious when the lateral displacement is large.
(2) Although RC-2, whose stirrups' weight loss is small, attains increases in strength and deformation capacity, the degree of intensity attenuation is greater than that of RC-1, whose stirrups lost no weight.
(3) The intensity attenuation of specimens with greater stirrup spacing is faster with the same weight loss of stirrups.

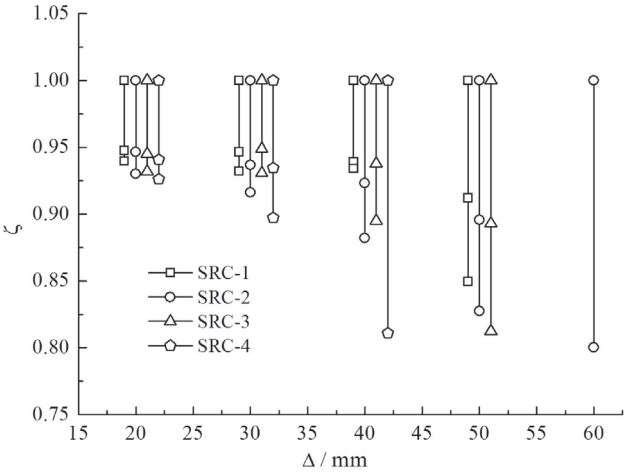

(a) Stirrup spacing 70mm

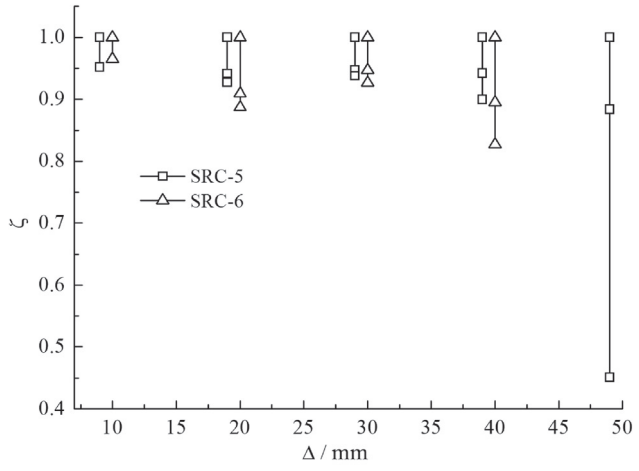

(b) Stirrup spacing 90mm

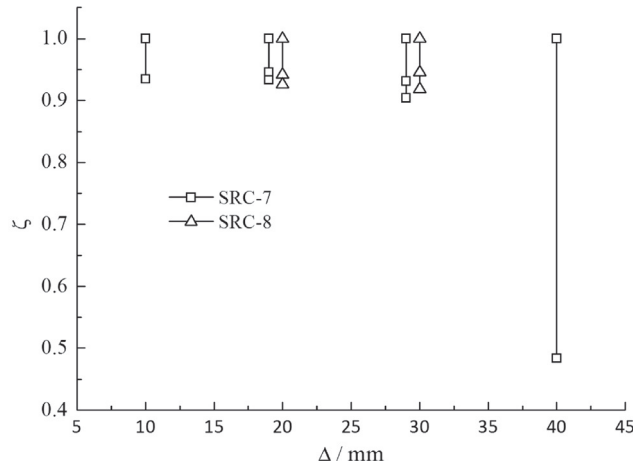

(c) Stirrup spacing120mm

Fig. 6. The influence on intensity attenuation of stirrup corrosion.

3.5. Stiffness degradation

To study the variation of reinforced concrete columns' stiffness degradation under low cyclic loading, the average stiffness of each stage of cyclic loading is expressed as follows:

$$K_i = \frac{|P_i| + |-P_i|}{|\Delta_i| + |-\Delta_i|}. \quad (1)$$

Fig. 8 depicts the average stiffness-deterioration curves of eight concrete columns.

Comparing the curves of specimens' stiffness degradation, the variation of reinforced concrete columns' stiffness attenuation can be described as follows:

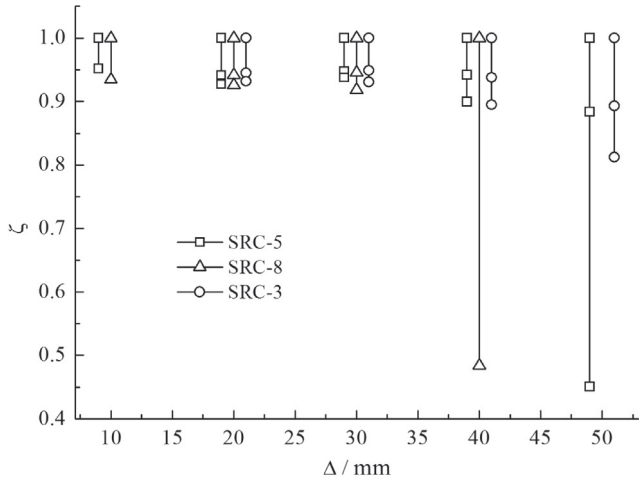

(a) The weight loss about 35%

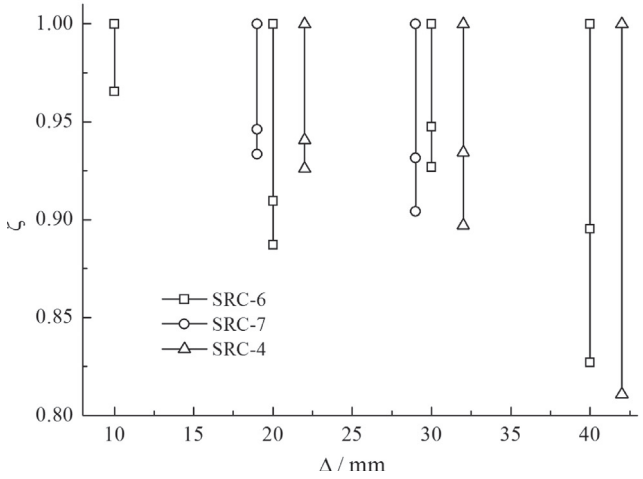

(b) The weight loss about 45%

Fig. 7. The influence on intensity attenuation of stirrup spacing.

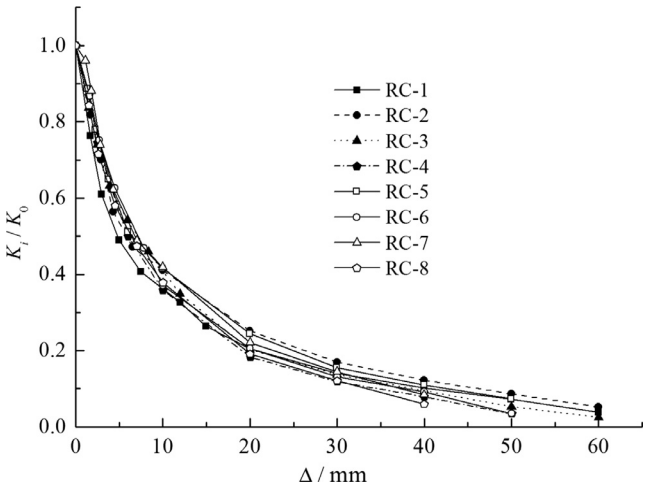

Fig. 8. Total energy dissipation of the corroded column.

(1) The variation of stiffness deterioration and the speed of stiffness degradation of all specimens are substantially the same. The stiffness deterioration of all specimens declines rapidly under a small lateral displacement, but the speed of stiffness deterioration is slower, and it levels off at last with continuous development of the plastic deformation and lateral displacement. The entire stiffness deterioration is more even, with no obvious stiffness mutation.
(2) RC-2 has less stiffness deterioration amplitude than RC-1 under the same displacement, which shows that slight corrosion of stirrups is beneficial to seismic performance.
(3) Differences in stiffness deterioration of specimens exist under different stirrup spacings. When the stirrup spacing is 70 mm, the stiffness deterioration amplitude of severely corroded specimens is less than that of RC-1 before transverse reinforcement yield. After transverse reinforcement yield, concrete cover cracking and the failure of work, internal forces released by concrete gradually transfer to the reinforcing bar, and confinement of the core concrete by corroded stirrups is gradually strengthened, the weakening effect of confinement to the core concrete by corroded stirrups appears gradually, stiffness degradation amplitude of severe corrosion is greater than for RC-1, and the amplitude increases with the rate of stirrup corrosion. When stirrup spacing is 90 mm or 120 mm, stiffness degradation is basically the same, and the amplitude increases with the rate of stirrup corrosion.

3.6. Ductility analysis

Ductility is an important parameter characterizing the deformation ability of structural members. It is usually expressed in the ductility coefficient. The displacement ductility coefficient usually refers to the ratio of the corresponding displacement when a skeleton curve decreases to $0.85F_{max}$ and the yield displacement. Its expression is $\mu = \Delta_u/\Delta_y$, where μ is the displacement ductility factor, Δ_u is the limit displacement, Δ_y is the yield displacement, and the yield point position is determined by the area of reciprocal method [13,14].

Supposing Δ/H is the relative deformation, Δ is displacement of the top lateral displacement of reinforced concrete columns, and H is the height of reinforced concrete columns. The peak load point, limit point, and other feature points corresponding to the load value, displacement ductility factor, and ultimate sway angle of every specimen in the test are shown in Table 7.

It can be seen from Table 7 that ductility exhibits the following behavior:

(1) The displacement ductility coefficient of the eight specimens is in the range of 3.05–4.08, and every specimen has good ductility. In descending order of ductility, the specimens are RC-2, RC-1, RC-3, RC-4, RC-5, RC-6, RC-7, and RC-8.
(2) Compared with RC-1, the ductility of RC-2 has increased, mainly because of stirrup corrosion product filling the voids between reinforcing steel and the surrounding concrete pore, which not only increases the compactness, but enhances the bond performance between steel bar and concrete.
(3) For specimens with similar amounts of stirrup corrosion, the stirrup spacing is smaller, the ductility of stirrups is greater, and the ultimate displacement angle is greater, indicating that stirrup spacing decreases are good for ductility.

Table 7
Characteristic parameters and ductility coefficient.

Specimens	Cracking		Yielding		Limiting		Ductility coefficient	Relative deformation	V_u/kN	V_p/kN	V_u/V_p
	V_K/kN	Δ_K/mm	V_y/kN	Δ_y/kN	V_w/kN	Δ_w/mm					
RC-1	53.92 −63.55	9.21 −12.68	63.81 −74.04	19.95 −30.06	56.43 −66.63	40.62 −45.12	3.92	1/21.9	68.93	65.24	1.056
RC-2	63.39 −65.48	9.35 −12.91	73.76 −78.32	19.98 −40.01	66.38 −70.49	38.20 −52.63	4.08	1/20.7	76.04	70.56	1.078
RC-3	56.95 −68.44	9.62 −12.11	65.97 −75.91	12.01 −30.03	59.37 −68.32	36.66 −46.58	3.88	1/22.3	70.94	69.18	1.025
RC-4	56.61 −60.85	9.52 −9.95	65.15 −68.27	20.03 −19.98	58.63 −61.44	32.81 −41.86	3.84	1/25.2	66.71	69.71	0.957
RC-5	56.37 −55.85	6.69 −14.24	65.56 −68.05	19.97 −30.04	59.01 −61.24	32.87 −45.82	3.59	1/23.9	66.81	68.08	0.981
RC-6	46.58 −60.75	9.11 −13.53	55.16 −71.15	20.01 −20.02	49.64 −64.04	30.36 –	3.33	1/31.0	63.16	66.66	0.947
RC-7	56.11 −56.26	8.65 −11.28	65.68 −66.72	20.01 −30.01	59.11 −60.05	32.82 −31.22	3.21	1/29.4	66.20	68.64	0.964
RC-8	46.53 −69.69	9.13 −12.96	54.52 −78.82	20.00 −20.01	49.07 −70.94	36.54 −30.74	3.05	1/26.9	66.67	67.69	0.984
										Mean	0.999

Note: (1) "+" indicate push load-in, "−" indicate tension load. (2) Average value in two directions is used in ductility coefficient, relative deformations.

(4) For specimens with the same stirrup spacing, the ductility decreases and the limit lateral angle increases as the corrosion rate of stirrups increases.

3.7. Energy-dissipation capacity analysis

The energy-dissipation capacity is an important index to measure the seismic performance of structures. Under a certain intensity, the structure can consume most of the energy in an earthquake and achieve a good anti-seismic effect if it has good energy-dissipation capacity. The total energy-dissipation capacity of the different stages of a member is used to evaluate the energy dissipation of members in the test.

In a low-reversed cyclic loading test, a contrastive analysis of the accumulated energy dissipation δ in the various control displacements of all specimens is shown in Fig. 9.

Through comparison and analysis, we can observe the following:

(1) After a member yields, the energy area gradually increases as load cycles increase. In the same control displacement cycle, energy dissipation of the second and third cycles is far less than that of the first cycle.
(2) For specimens with the same stirrup spacing, the total energy dissipation of RC-2 when corroded slightly is greater than that of RC-1, and the total energy dissipation capacity of other specimens before serious damage is significantly lower than that of RC-1. The total energy dissipation of all specimens decreases gradually as the weight loss of stirrups increases, which shows that the energy-dissipation capacity decreases because of stirrup corrosion.
(3) For specimens with different stirrup spacing, the decline of total energy-dissipation capacity increases gradually at different levels as the weight loss of stirrups increases. The amplitude of total energy-dissipation capacity decreases as the weight loss of stirrups increases and the stirrup spacing decreases.
(4) The total energy dissipation of RC-2 when corroded slightly is greater than that of RC-1 under every control displacement, which shows that slight corrosion of stirrups is good for energy-dissipation capacity. In other, less seriously corroded specimens, the amounts of energy dissipation and cumulative energy dissipation are greater than those of RC-1 under the same control lateral displacement in the elastic-plastic stage, which shows that the bonding-enhancement effect between reinforcement and concrete is obvious in the low-reversed cyclic loading test, and is also good for seismic capacity.

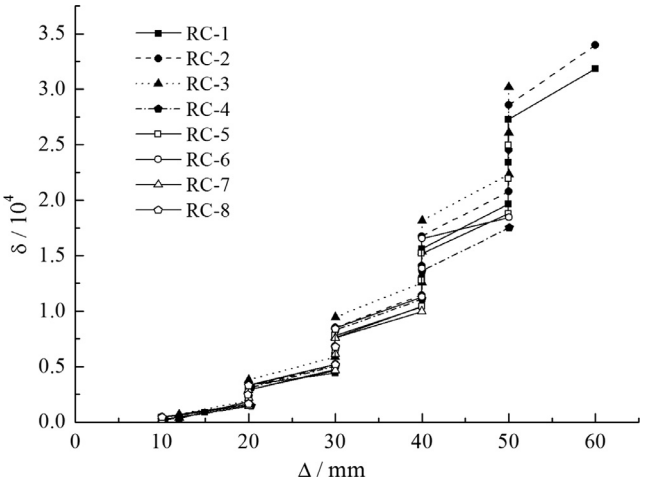

Fig. 9. Total energy dissipation of the corroded column.

4. Prediction of the lateral strength

Under low-reversed cyclic loading, corroded reinforced concrete columns work as compression-bending members. Therefore, a method for prediction of the lateral strength of reinforced concrete columns confined by corroded stirrups is presented based on the axial-shear-flexure interaction (ASFI) approach [15] for conventional concrete columns, with modification to consider the effect of stirrup corrosion.

4.1. Axial-shear-flexure interaction approach

As shown in Fig. 10, the axial-shear-flexure interaction approach consists of two interactive models referred to as the axial-flexure model and axial-shear model. The axial-flexure model is based on cross-sectional analysis, and the axial-shear model is based on modified compression field theory.

To link the two interactive models, equilibrium between the axial-flexure and axial-shear models should be strictly satisfied by imposing the same shear force (V) and axial force (P) to both models at any step during analysis. The shear stress τ_s in the axial-shear model is obtained by $V/(b_w d_s)$, where b_w is the width of the column section and d_s is the depth of the column section, which usually equals the overall depth of the section (h) before concrete cracking in flexure, and the effective depth of the section (d) after cracking. The normal stress in the x direction (σ_x) of the axial-shear models is equal to the stress induced by the axial load. The normal stress in the y and z directions of the axial-shear model is assumed to be zero. It should be noted that compatibility between the axial-flexure and axial-shear models is satisfied by requiring the axial strain caused by the axial mechanism in both models to equal that caused only by the axial load.

In the axial-shear-flexure interaction method, the equilibrium and compatibility conditions should be satisfied as with any theo-

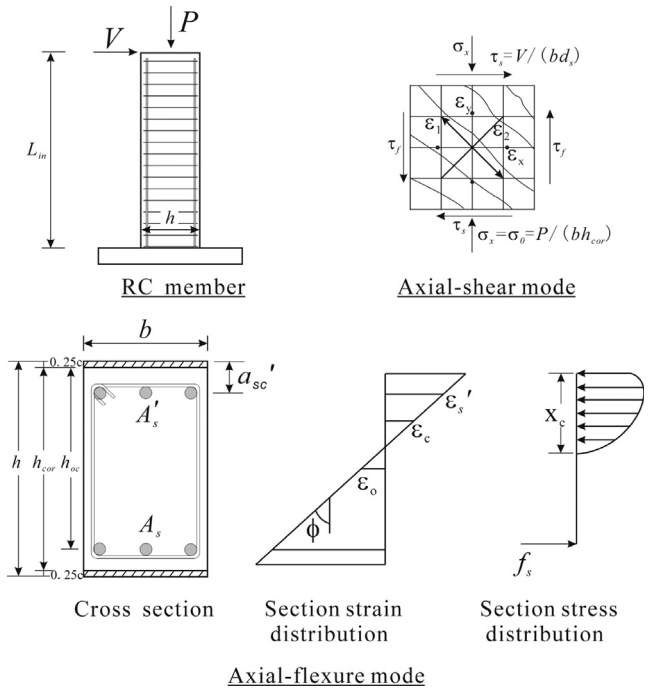

Fig. 10. The axial-shear-flexure interaction approach.

retical model. In particular, the average compressive strains of concrete should meet the deformation compatibility condition. The axial strain caused by the flexural mechanism (ε_{xf}) in the axial-flexure model is added to the axial strain in the axial-shear model ($\varepsilon_{xa} + \varepsilon_{xs}$). Therefore, the axial strain ε_x in the ASFI approach becomes the sum of ε_{xf}, ε_{xa}, and ε_{xs}.

For a reinforced concrete cantilever column, the concrete principal compressive strain ε_2 between two cross-sections is the average principal compressive strain of the element between the two adjacent sections i and $i+1$. Thus,

$$\varepsilon_2 = 0.5(\varepsilon_{2_i} + \varepsilon_{2_{i+1}}). \tag{2}$$

Another key issue is the compression softening coefficient, which is used in the axial-shear model to soften diagonally cracked concrete in compression. Normally, the compression softening coefficient ξ is obtained by

$$\zeta = \frac{1}{0.8 - 0.34\varepsilon_1/\varepsilon_c'} \le 1.0, \tag{3}$$

where ε_c' is the strain at the peak stress of concrete in compression, taken as 0.002; and ε_1 is the average concrete principal tensile strain determined from the axial-shear model.

4.2. Effect of stirrup corrosion

Generally, the corrosion of steel reinforcement will cause material property degradation, geometric changes, and bond degradation of concrete members. In this section, the effect of stirrup corrosion on the lateral strength of reinforced concrete columns mainly focuses on the material property degradation and geometric changes of stirrups, since there is limited information on the bond degradation model for corroded reinforced concrete structures.

The stress-strain relationship of steel reinforcement under tension is modeled based on the Mander model as shown below:

$$f_s = \begin{cases} E_s\varepsilon_s & \text{for } \varepsilon_s \le \varepsilon_{sY} \\ f_{sY} + 0.02E_s(\varepsilon_s - \varepsilon_{sY}) & \text{for } \varepsilon_{sY} \le \varepsilon_s \le \varepsilon_{sh} \\ f_{su} + (f_{sh} - f_{su})\left(\frac{\varepsilon_{su} - \varepsilon_s}{\varepsilon_{su} - \varepsilon_{sh}}\right)^2 & \text{for } \varepsilon_{sh} \le \varepsilon_s \le \varepsilon_{su} \end{cases} \tag{4}$$

where f_s and ε_s are the stress and strain of steel reinforcement, respectively; f_{sY} and ε_{sY} are the yield stress and strain of steel reinforcement, respectively; f_{sh} and ε_{sh} are the stress ($f_{sh} = f_{sY} + 0.01E_s(\varepsilon_{sh} - \varepsilon_{sY})$) and strain at the starting point of hardening, respectively; f_{su} and ε_{su} are the ultimate stress and strain of steel reinforcement, respectively; and E_s is the modulus of elasticity of steel reinforcement.

Once the stirrups are corroded, the effective cross-sectional area of steel reinforcement will reduce. By assuming a uniform reduction occurs in the cross-sectional area along the length of corroded bars, the reduced cross-sectional area of corroded stirrups is given by

$$A_s(\Delta w) = \frac{\pi D_0^2}{4}(1 - 0.01 \times \Delta w) \tag{5}$$

where $A_s(\Delta_w)$ is the cross-sectional area of a corroded bar; Δw is the average corrosion mass loss (%); and D_o is the uncorroded bar diameter.

The yield strength f_{yc} of the corroded stirrups can be obtained by

$$f_{yc} = (1 - \beta \times \Delta w) f_{y0} \tag{6}$$

where f_{yc} is the corroded yield strength; β is the strength reduction factor, taken as 0.005; and f_{y0} is the uncorroded yield strength.

4.3. Procedures for estimation of lateral strength

The failure modes of all the experimental specimens are shown in Table 6. Three failure modes are observed as shear failure at a crack (mode 1), concrete crushing (mode 2), and flexure-shear failure (mode 3).

Shear failure occurs when the following conditions are met:

$$\tau_f = \frac{M}{bd_fL_{in}} \ge \tau_i + f_{syy}\rho_{sy}\cot\theta \tag{7}$$

where $d_f = h_{0c}$.

If corroded reinforced concrete columns do not fail via mode 1 (shear failure), concrete crushing failure may occur, and then

$$\tau_f = \frac{M}{bd_fL_{in}} \ge \frac{f_{c1} - f_{c2}}{\tan\theta + \cot\theta} \tag{8}$$

where $d_f = h_{cor}$ for shear span ratios less than 1, and $d_f = h_{0c}$ for shear span ratios greater than 1.5. If the shear span ratio is between 1.0 and 1.5, d_f is obtained through linear interpolation.

With a relatively higher stirrup ratio and excellent ductility, RC columns will fail in shear when $\varepsilon_2 = \varepsilon_c'$, and

$$\tau_f = \frac{M}{bd_fL_{in}}, \tag{9}$$

where $d_f = h_{cor}$.

The ultimate lateral strength of corroded reinforced concrete columns can be calculated by the following procedures.

1) According to Eqs. (5) and (6), the residual cross-section and yield strength of corroded reinforcement bars can be calculated.
2) The geometric parameters of the specimen should be reduced due to the geometric damage of the corroded specimens, such as the depth of the section $h_{cor} = h - c/2$, where c is the thickness of concrete cover; and effective sectional depth $h_{0c} = h_{cor} - D/2 - c/2$, where D is the diameter of the longitudinal steel.
3) Assume that the initial value of concrete compressive strain ε_c is ε_c'.
4) The centroidal strain ε_0 is solved by

$$\varepsilon_0 = \frac{h_{cor}P - 1.7391h_{cor}[A_s'E_s' + A_sE_s + abE_c]\varepsilon_c}{2[a_{sc}'A_s'E_s' + h_{0c}A_sE_s + 0.5bE_ca^2]} + 1.7391\varepsilon_c \tag{10}$$

5) The axial compressive strain ε_{xa} at the inflection point is calculated by

$$\varepsilon_{xa} = \frac{P/bh_{cor}}{2f_p/\varepsilon_p + E_s\rho_{sx}}, \tag{11}$$

where f_p and ε_p represent the peak stress and strain of confined concrete, respectively, which is taken as $f_p = f_c'$, $\varepsilon_p = \varepsilon_c'$.
6) Calculate the average principal compressive strain $\varepsilon_2 = (\varepsilon_c + \varepsilon_{xa})/2$, and the x-direction strain $\varepsilon_x = (\varepsilon_0 + \varepsilon_{xa})/2$, of concrete.
7) Determine the y-direction strain ε_y:

$$\varepsilon_y = \sqrt{b^2 + c} - b, \varepsilon_y < \varepsilon_{yy}, \tag{12}$$

where $b = \frac{f_{c1}}{2\rho_{sy}E_s} - \frac{\varepsilon_2}{2}$ and $c = \frac{(\varepsilon_x - \varepsilon_2)(f_{c1} - f_{cx}) + f_{c1}\varepsilon_2}{\rho_{sy}E_s}$.

The stirrups always yield when the specimen fails, and then Eq. (13) can be used for calculation:

$$\varepsilon_1 = \frac{(\varepsilon_x - \varepsilon_2)(f_{c1} - \sigma_x + \rho_{sx}E_s\varepsilon_x)}{(f_{c1} + \rho_{sy}f_{syy})} \tag{13}$$

where $\sigma_x = \sigma_0 = P/(bh_{cor})$ and $f_{c1} = 0.44f'_v = 0.44 \times 0.33\sqrt{f'_c}$.

8) Solve Eq. (14) to obtain the value of θ;

$$\tan^2\theta = \frac{\varepsilon_x - \varepsilon_2}{\varepsilon_y - \varepsilon_2} = \frac{\varepsilon_1 - \varepsilon_y}{\varepsilon_1 - \varepsilon_x} \quad (14)$$

9) Use Eqs. (7) through (9) to check for shear failure. If it occurs, then reduce ε_c and repeat the above steps until inequality 7 is within 5% on both sides.
10) If shear failure does not occur, use Eq. (8) to check whether the cover concrete is crushed.
11) If Eqs. (7) and (8) are both untenable, indicating that the corroded specimens have experienced flexure shear failure, the stress τ_f can be calculated through Eq. (9).
12) Finally, the ultimate lateral load V_u is obtained by

$$V_u = \tau_f bh_{cor} \quad (15)$$

4.4. Model validation

The suggested theoretical model based on MATLAB numerical software was validated by comparing predicted lateral strength and lateral bearing capacity of uncorroded and corroded concrete columns with axial loads. The comparisons between predicted values and experimental results are shown in Table 7. The average ratio of experimental values to predicted values of lateral bearing capacity is 0.999, showing that analytical results agree well with the experimental values.

5. Conclusions

Through the low-reversed cyclic loading test of concrete columns confined by corroded stirrups, a contrast analysis of the failure process, the failure pattern, hysteresis performance, and energy-dissipation capacity has been carried out, leading to the following conclusions.

(1) Due to the effect of corrosion on bonding enhancement between the reinforcement and concrete, the seismic performance of the concrete column is not degraded but improved when stirrup corrosion is slight.
(2) When stirrups suffer serious corrosion, the confinement effect on the core concrete and transverse reinforcement is weakened, the seismic behavior of the columns is reduced, and the damage feature points that appears in the process of destruction is advanced. Meanwhile, the failure mode gradually changes from ductile failure to brittle failure as the weight loss of the stirrups increases.
(3) With the increasing weight loss of the stirrups, the ductility and total energy-dissipation capacity of reinforced concrete columns decreases, and the degree of decline is related to the degree of confinement of the corroded stirrup. The greater the degree of confinement of a concrete column by stirrups, the greater is the degree of degradation of the ductility coefficient and total energy-dissipation capacity after stirrup corrosion.
(4) For concrete columns confined by seriously corroded stirrups, the amount of energy dissipation and cumulative energy dissipation is greater than for RC-1 under the same control lateral displacement in the elastic-plastic stage.
(5) A lateral strength-prediction method is proposed for reinforced concrete columns confined by corroded stirrups. There is good agreement between the test results and theoretical values.

Acknowledgments

This outcome has been achieved with the financial support of the National Youth Science Fund of China (Project No. 51408483, Name: The shear performance research on corroded reinforced concrete column) and the Natural Science Fund of Shaanxi Province (Project No. 2017JM5045, Name: Study on seismic behavior of corroded reinforced concrete columns). Meanwhile, We thank LetPub (www.letpub.com) for its linguistic assistance during the preparation of this manuscript.

References

[1] M. Setzer, R. Augberg, H.J. Keck, Frost Resistance of Concrete, Rilem Publications, Essen, Germany, 2002.
[2] Di-tao Niu, Durability and Life Prediction of Concrete Structures, Science Press, Beijing, 2003.
[3] J.S. Kong, D.M. Frangopol, Life-cycle reliability-based maintenance cost optimization of deteriorating structures with emphasis on bridges, J. Struct. Eng. 129 (6) (2003) 818–828.
[4] Weiliang Jin, Ditao Niu, The state-of-the-art on durability and life-cycle design theory of engineering structures, Eng. Mech. 28 (9) (2011) 31–37.
[5] Ditao Niu, Xinxiao Chen, Xuemin Wang, Experimental research on seismic performance of corroded R. C. members, Build. Struct. 34 (10) (2004) 36–39.
[6] Jinxin Gong, Weiqiu Zhong, Guofan Zhao, Experimental study on low-cycle behavior of corroded reinforced concrete member under eccentric compression, J. Build. Struct. 25 (5) (2004) 92–97. 104.
[7] Jinbo Li, Jinxin Gong, Influences of rebar corrosion on seismic behavior of circular RC columns, China J. Highway Transp. 21 (4) (2008) 55–60.
[8] Lianjie Jiang, Yingshu Yuan, Experimental study on mechanical behavior of corroded reinforced concrete column under cyclic loading, Ind. Constr. 42 (2) (2012) 66–69. 13.
[9] Xiudai Fu, Feng Ma, Yongzhe Yang, Experimental study of lattice composing shear wall seismic performance, J. Tianjin Univ. 33 (3) (2000) 336–340.
[11] Qi Li, Jiajie Wu, Experimental study of L-shaped section steel reinforced concrete columnunder low reversed cyclic loading, Build. Struct. 41 (1) (2011) 11–13.
[12] Greifenhagen Christian, Lestuzzi Pierino, Static cyclic tests on lightly reinforced concrete shear walls, Eng. Struct. 27 (11) (2005) 1703–1712.
[13] Shansuo Zheng, Bin Wang, Fei Yu, et al., Experimental study on damage of SRC frame beams under low cycle reversed loading, Eng. Mech. 28 (7) (2011) 37–44.
[14] T.N. Salonikios, A.J. Kappos, I.A. Tegos, Cyclic load behavior of low-slenderness reinforced concrete walls: design basis and test results, ACI Struct. J. 96 (4) (1999) 649–660.
[15] H. Mostafaei, T. Kabeyasawa, Axial-shear-flexure interaction approach for reinforced concrete columns, ACI Struct. J. 104 (2) (2007) 218–226.